Journal of the National Academy of Forensic Engineers®

http://www.nafe.org
ISSN: 2379-3252

Vol. 33 No. 1 June 2016

Advanced Forensic Engineering Analysis of a School Bus/Tractor-Trailer Crash

By Richard M. Ziernicki, PhD, PE (NAFE 308F) and William H. Pierce, PE (NAFE 846C), and Angelos G. Leiloglou, M. Arch. (NAFE 956C)

Abstract

This paper presents advanced techniques used to reconstruct a motor vehicle accident involving a fully loaded tractor-trailer and school bus with 30 young students. The accident investigation included analysis of the physical evidence using photogrammetry and high-definition laser scanning, application of engine control module (ECM) and global positioning system (GPS) data, and analyzing onboard video footage from the bus. Momentum-based crash simulation software (PC-Crash) was used to simulate the accident. The simulation data was compared with National Transportation Safety Board (NTSB) data and with the onboard bus video footage. Further, rigid-body kinematic equations were used to determine occupant kinematics (velocities) and dynamics (accelerations). Multiple graphics are used to demonstrate the accident reconstruction and occupant kinematics and dynamics.

Keywords

School bus, tractor-trailer, on-board video, photo-match, rigid-body kinematics, PC-Crash, point clouds, photogrammetry, high-definition scanning, interactive animation, event data recorder

Introduction

A school bus loaded with 30 children was traveling westbound on a four-lane divided highway. The school bus proceeded to turn left across the eastbound lanes of the divided highway, approaching a two-lane divided road. However, the bus was crossing the eastbound lanes of the divided highway into the path of a tractor-trailer, which was carrying a load of sod.

The semi driver applied the brakes, but was unable to avoid colliding with the rear right side of the school bus. As a result of the collision, the school bus spun clockwise (approximately 180 degrees in yaw) prior to coming to rest near the northbound lane of the divided two-lane road. The semi came to rest in a ditch east of the school bus with the semi-tractor rolling a quarter turn and semi-trailer rolling a half turn.

According to the National Transportation Safety Board (NTSB), 11 children sustained minor injuries, eight children sustained major injuries, and there was one fatality. The lead author of this paper was retained to reconstruct the accident by the law firm representing the family of the child that was fatally injured.

In addition, 21 of the 29 surviving children on the bus responded to a general accident questionnaire issued by the NTSB. All of those 21 children reported wearing lap belts at the time of the accident. Further, there was evidence that the fatally injured child was wearing his seatbelt at the time of the accident. However, the fatally injured occupant's lap belt unlatched during the incident, and his seat cushion became detached. The victim was found in the aisle near the rear of the bus.

This paper presents several technologies and methodologies used to reconstruct and animate the accident. The reconstruction of the accident involved reviewing NTSB's accident investigation; analysis of physical evidence; estimating impact speeds and post-impact speeds from NTSB investigation, on-board school bus video footage, school bus global positioning data, and the semi's engine control module; simulating the accident using PC-Crash; verifying the simulation data using on-board school bus video; determining the kinematics throughout the school bus; and finally creating photo-realistic animation and interactive animation of the accident.

NTSB Investigation Summary

During the accident investigation, the NTSB performed high-definition scanning of the accident site, the semi, and the school bus, evaluated the injuries sustained by all of the passengers on the school bus, and conducted an occupant kinematics study to evaluate the

Richard Ziernicki, PhD, PE, and William Pierce, PE, 7185 South Tucson Way, Englewood, CO 80112-3987
(303) 925-1900; rziernicki@knottlab.com, wpierce@knottlab.com

effectiveness of lap belts using Mathematical Dynamic Models (MADYMO) software.

The authors of the paper expanded upon NTSB's investigation by determining impact configuration, reconstructing speeds of both vehicles prior to, during, and after the collision, simulating the accident, and preparing an occupant kinematics model without relying on expensive MADYMO software.

Physical Evidence

Reconstruction of the accident first involved plotting the physical evidence. The Florida Highway Patrol (FHP) surveyed the accident scene, which included several tire marks. The authors of this paper identified additional evidence on the roadway using scene photographs. After identifying the additional evidence, photogrammetry was performed using police photographs to identify the locations of the physical evidence (**Figure 1**). **Figure 2** shows the evidence placed on a scaled diagram.

Figure 1
Photogrammetry of tire marks.

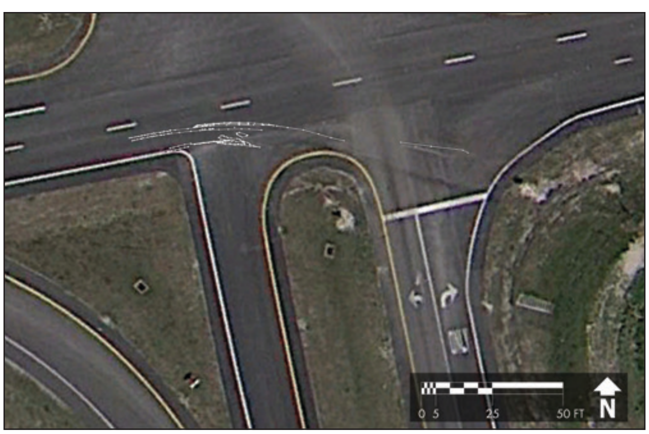

Figure 2
Physical evidence overlaid on aerial diagram.

After plotting the physical evidence, the authors determined the impact configuration. First, photographs were taken around the perimeter of the school bus. Photogrammetry software (Photomodeler Scanner) was used to create a 3-dimensional model of the damaged school bus in virtual space (**Figure 3**). Further, the geometry of the semi-tractor was captured using a high-definition 3-D laser scanner, in which 3 million points of the semi-tractor were captured (**Figure 4**).

Figure 3
Point Cloud of exterior of subject school bus.

Figure 4
Point Cloud of exterior of subject semi.

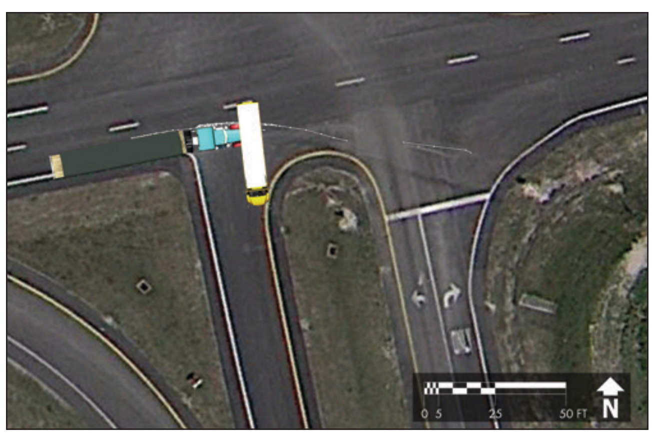

Figure 5
Impact configuration overlaid on physical evidence diagram.

Next, the virtual bus and semi-tractor models were aligned such that their crush profiles matched, thus establishing the impact configuration. The bus and semi-tractor impact configuration were then overlaid on top of the physical evidence diagram (**Figure 5**).

Figure 6
School bus GPS data plotted on aerial image.

The physical evidence shows at least 14 feet of skid marks left by the semi-tractor's left rear tires prior to impact, indicating that the semi-tractor had locked brakes before impact. After impact, scrub marks were left by the rear wheels of the school bus, showing rotational yaw motion of the school bus. The left-side bus tires dug into the grassy median as the bus spun, as evidenced by the deep furrow marks. The semi-trailer overturned as the semi-tractor entered the ditch on the southeast corner of the intersection, as evidenced by the sod dirt and gouges in the road.

Impact Speed Analysis

The pre-impact speeds of the school bus and the semi were approximated using data obtained by the FHP and NTSB. The pre-impact speeds determined through this analysis were used as starting points during momentum-based simulation of the accident using PC-Crash. More accurate pre-impact speeds of the school bus and semi were determined through the simulation of the accident, which will be discussed later in the paper.

The school bus had an onboard global positioning system (GPS) that recorded the location and instantaneous speed of the bus every 15 seconds. The authors used the GPS data to plot the position and corresponding instantaneous speed of the school bus every 15 seconds in the one minute prior to the collision (**Figure 6**). The last recorded GPS data point occurred near the point of impact. At this point, the bus was traveling at 15 mph. Therefore, the speed of the bus in the vicinity of the impact was 15 mph. The spatial resolution of the GPS introduces some error. However, this speed was used as a starting point during simulation of the accident in PC-Crash.

In order to approximate the pre-impact speed range of the semi, the authors relied on both the semi's event data recorder (EDR) and the onboard school bus camera that was pointed near the steps of the bus.

One of the onboard school bus cameras was pointed toward the steps of the bus recording at 15 frames per second. Five frames prior to noticeable movement due to impact, the semi came into frame near the southwest corner solid edge line of the roadway (**Figure 7**). Based on the frame rate, the semi came into frame between 0.26 and 0.33 seconds prior to impact. The impact configuration diagram shown in **Figure 5** was used to determine that the semi was 20.8 feet from the impact location between 0.26 and 0.33 seconds prior to impact.

Figure 7
Semi comes into view of bus camera five frames prior to impact.

Further, skid marks indicate that the semi was braking at least 14 feet prior to impact, and the EDR data indicated that the semi was decelerating at a rate of 0.316 g's prior to impact. Using the distance, time range, and deceleration rate of the semi, the authors were able to determine the impact speed range of the semi.

The impact speed range of the semi was determined to be 42 to 53 mph using this analysis (calculations shown in **Appendix A**). The impact speed range of the semi was further refined by incorporating the semi's EDR data, which recorded the semi speed in one-second intervals.

Based on the EDR data (**Figure 8**), the semi had the brakes applied and decelerated at an average constant rate of 0.319 *g* to 49 mph or less. The constant average deceleration rate with application of brakes is consistent with braking and no impact. Between 37 and 49 mph, the average deceleration rate increased to 0.546 *g*, consistent with the semi impacting the bus between 37 and 49 mph.

The EDR data showed that impact occurred after the semi decelerated to 49 mph or less, and the video analysis showed the semi's pre-impact speed was at least 42 mph. Therefore, the range of the semi's pre-impact speed was between 42 and 49 mph.

Post-Impact Speed Analysis

Next, the post-impact speeds — or the speeds of both the semi and the school bus after maximum engagement — were approximated. The post-impact speeds were later refined during simulation of the accident using PC-Crash. The authors used the NTSB video analysis bus position data to approximate the post-impact speeds of both the school bus and the semi.

First, the school bus speeds were plotted by differentiating the NTSB bus position data (**Figure 9**). Using this method, the bus separation speed was determined as approximately 28 mph. After estimating the school bus post-impact speed, the semi's post-impact speed was determined from the NTSB bus position data.

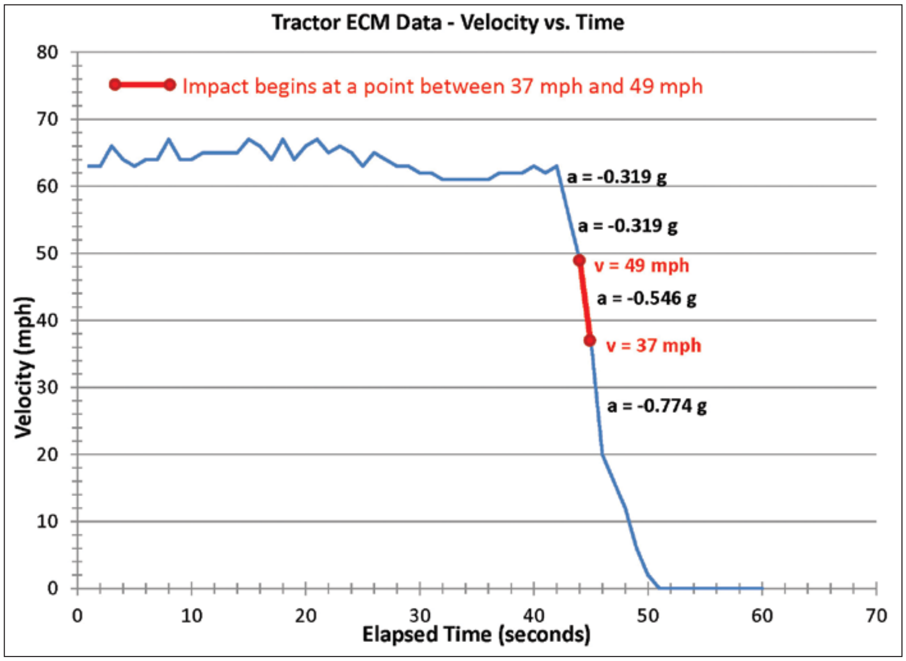

Figure 8
Plotted semi EDR data.

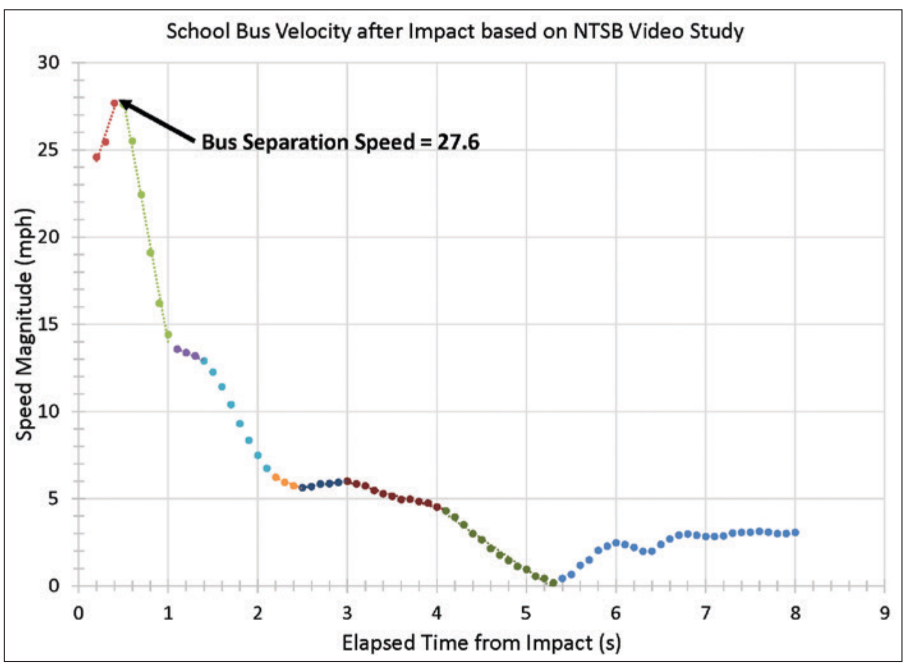

Figure 9
Post-impact bus speed determined from NTSB position data.
(The various colors shown are arbitrary.)

To calculate the semi's post-impact speed, the school bus position data from NTSB's video analysis was used to plot the location of the bus every 0.1 seconds through the impact sequence. The location of the point of maximum engagement on the bus was also plotted in 0.1-second intervals (**Figure 10**). This location corresponds to the approximate position of the front of the semi through impact. By differentiating the position data around the point of maximum engagement, the authors determined that the separation speed of the semi was approximately 36 mph.

PC-Crash Simulation

After determining the approximate pre- and post-impact speeds of both the school bus and the semi, the authors simulated the collision using momentum-based simulation software (PC-Crash).

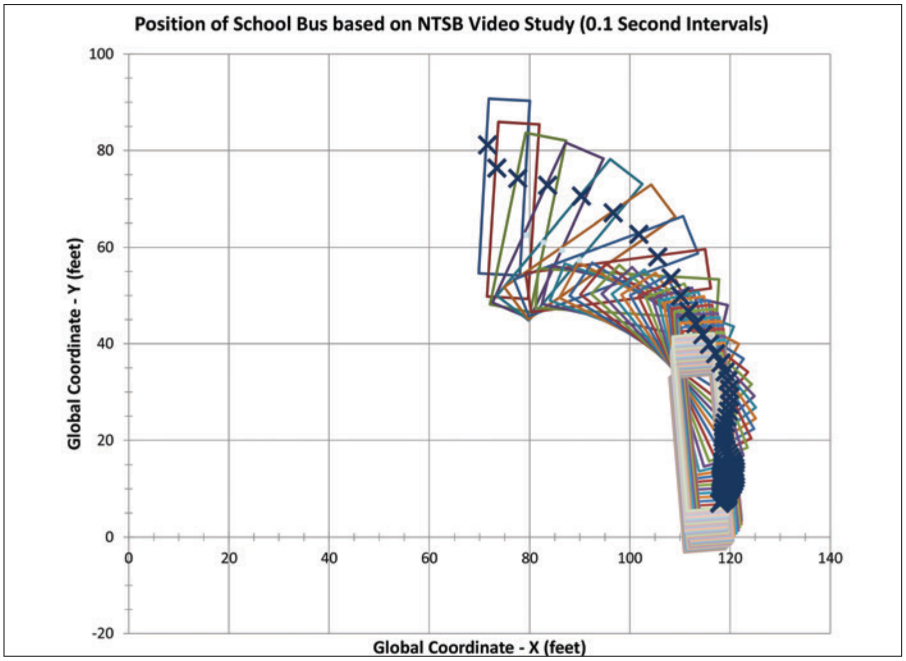

Figure 10
Bus position (0.1-second intervals) plotted from NTSB data.

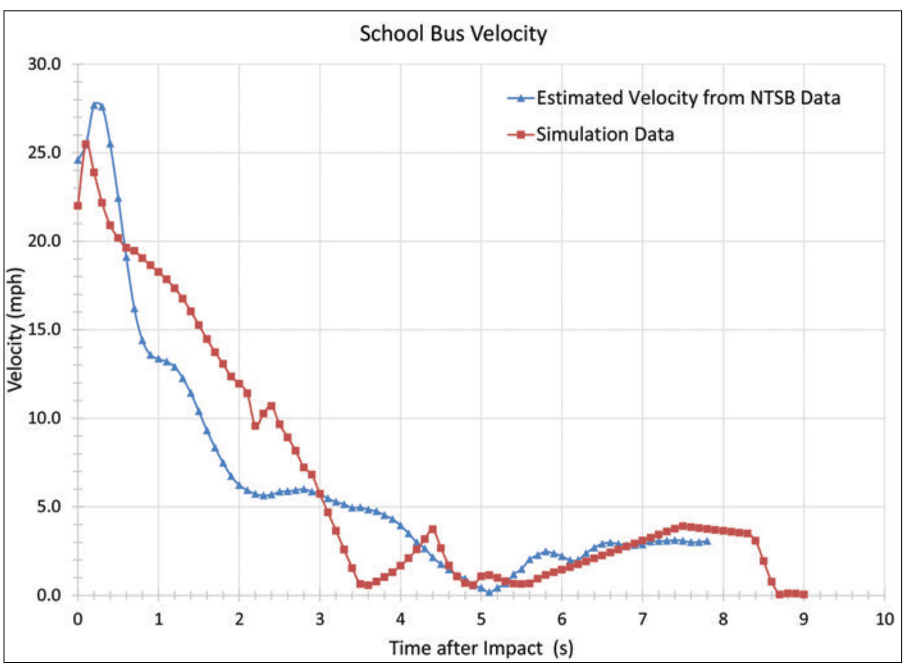

Figure 11
Bus post-impact speeds simulated in PC-Crash compared to NTSB video study.

The simulation process involved first determining the inertial parameters of both the school bus and semi as well as roadway friction properties. Virtual roadway terrain, physical evidence, and impact configuration were also input into PC-Crash.

After setting up the physical parameters and accident scene evidence in PC-Crash, the authors used the approximate pre-impact speeds of both the school bus and the semi as a starting point in the simulation process. The pre-impact speeds of both the school bus and the semi were refined by simulating the motion of both the school bus and semi until the motion of the school bus and the semi best matched the physical evidence and the approximated post-impact speeds of both the school bus and semi.

The PC-Crash simulation was used to determine a pre-impact speed of the school bus of 22 mph and the pre-impact speed of the semi of 45 mph. The simulation data further showed a post-impact speed of the school bus of 26 mph and a post-impact speed of the semi of 39 mph.

The PC-Crash speed of the school bus was then compared to the speeds determined through analysis of the NTSB data (**Figure 11**). Further, the PC-Crash simulation roll rate of the school bus was also compared to the roll rate obtained by the NTSB through video analysis. There was a high rate of consistency between the authors' PC-Crash simulation and the NTSB video analysis. As a further check for consistency, the simulation motion was applied to virtual models of the school bus and semi. A virtual school bus camera was placed in the location of the onboard school bus camera that was directed toward the steps and the door of the school bus. The simulated motion of the school bus and semi (as viewed through the virtual camera) closely matched the motion of the school bus and semi (as observed through the onboard school bus camera), thus further verifying the reliability of the PC-Crash simulation data.

Calculation of Delta-V at Seat of Fatally Injured

After simulating the accident, the authors investigated the delta-V vector — or change in velocity vector — at the seat of the fatally injured occupant.

The semi struck the side of the bus offset far from the bus's center of gravity, resulting in the bus sustaining a large post-impact rotational velocity. Due to the extended length of the bus, the authors hypothesized that the change in tangential velocity associated with the bus's rotational velocity had a significant effect on the overall change in velocity sustained by the bus near the seat of the fatally injured occupant, who was sitting near the rear of the bus.

In order to account for the change in rotational velocity at the seat position of the fatally injured occupant when determining overall delta-V, the principles of rigid body kinematics were applied.

The PC-Crash simulation data was used to determine the delta-V of the combined bus and bus occupants center of gravity (ΔV_B) and the change in rotational speed about the center of gravity ($\Delta\omega$). The distance vector from the bus's center of gravity to the fatally injured occupant seat position was also measured using a scaled bus schematic ($r_{A/B}$). The magnitude and direction of delta-V at the seating location of the fatally injured occupant was then calculated using the equation for rigid body kinematics:

$$\Delta V_A = \Delta V_B + \Delta\omega \times r_{A/B} \tag{1}$$

Figure 12 shows the graphical representation of the application of equation (1). The velocity components associated with roll and pitch rotational velocities were determined insignificant and therefore neglected. **Figure 13** shows the summary of the velocity components and magnitudes of both the CG and the location where the fatally injured occupant was sitting (roll and pitch rotational velocities neglected).

For reference, calculations (including roll and pitch rotational velocities) are provided in **Appendix B**. When accounting for roll and pitch rotational velocities, the magnitude of the delta-V for the location of the fatally injured occupant was 61.7 mph or 2.2 percent higher than when roll and pitch rotational velocities were neglected.

Figure 13 shows that the change in velocity of the center of gravity was only 22.5 mph whereas the change in velocity at the seating position of the fatally injured was significantly higher (60.3 mph). Therefore, the authors' hypothesis that the change in rotational velocity significantly affected the overall change in velocity at the seat location of the fatally injured was proven valid.

Variation of Delta-V throughout Bus

The authors also calculated (with the assistance of computing software) the magnitude of delta-V throughout the bus at seat level by applying equation (1) to thousands of points equally spaced at seat level height. The computing software was also used to create a color-coded diagram showing the delta-V throughout the bus at seat level. Further, the authors overlaid the NTSB occupant injury severity data over the color-coded delta-V diagram (**Figure 14**).

Figure 14 shows that the delta-V near the front of the bus was nearly 0 mph, whereas the delta-V increased approaching the rear of the bus with the rear of the school bus sustaining a delta-V near 70 mph. As expected, the general injury severity as categorized by the NTSB also increased toward the rear of the school bus. The significant variation in delta-V throughout the bus shows that the effects of rotation in offset collisions involving extended length passenger vehicles, such as buses or long vans, cannot be neglected.

Alternative Graphical Method to Determine Delta-V

After determining the delta-V vectors for two points using the equation of rigid body kinematics, a simple graphical method can be applied to quickly determine the speed and direction of the delta-V at any

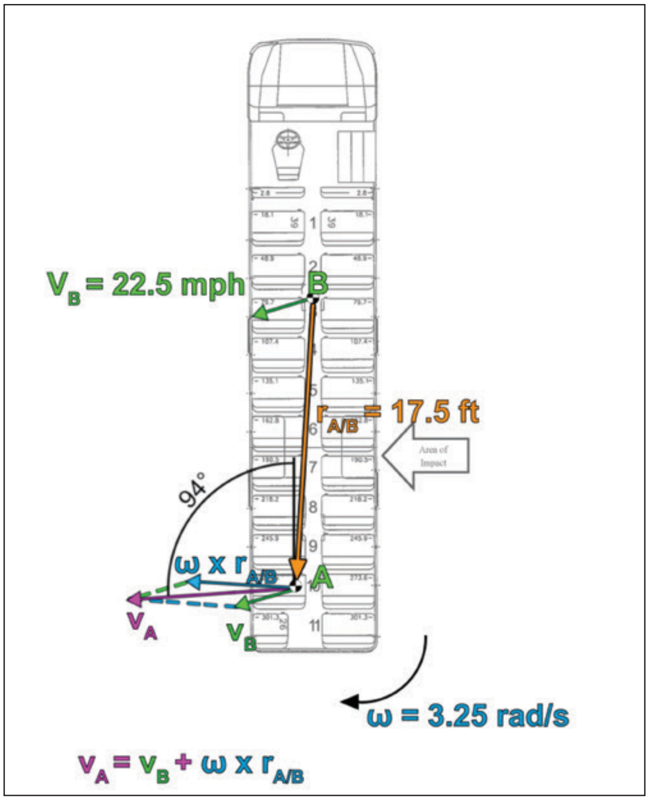

Figure 12
Graphical representation of rigid body kinematic calculations.

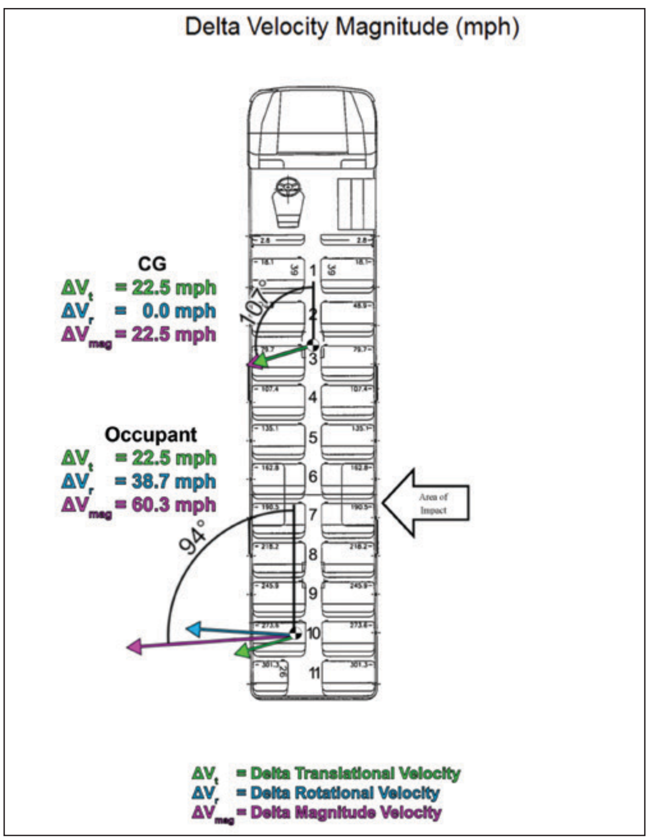

Figure 13
Summary of the velocity components of CG and seat of fatally injured occupant.

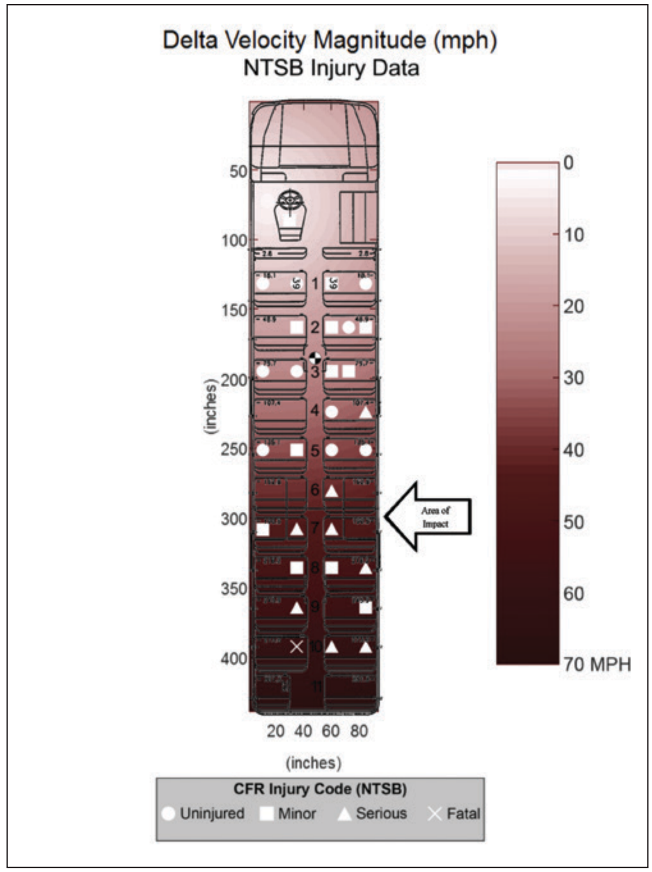

Figure 14
Magnitude of delta-V and reported injury severity.

point on the school bus in two-dimensional space. This graphical method neglects effects of the roll and pitch rotational velocities and therefore can only be used when the roll and pitch rotational velocities can be neglected, such as in this case study. The analysis first involves determining the instant center — or location on the bus in two-dimensional space — that sustained a delta-V of 0 mph. The instant center is determined by drawing perpendicular lines from the delta-V magnitude vectors of the CG and the fatally injured occupant. The point where the lines intersect is considered the instant center (**Figure 15**).

After determining the instant center, the delta-V vector at any section of the bus could be calculated. As an example, the delta-V sustained by the bus driver's seat was calculated; first the magnitude was determined. In order to calculate the magnitude of the delta-V, the distance from the instant center to the bus driver seat, $d_{drivers}$, and the distance from the instant center, d_{CG}, were determined (**Figure 16**). The magnitude of the delta-V for the bus driver seat was calculated using equation (2). The application of quantities in equation (2) is shown in equation (3).

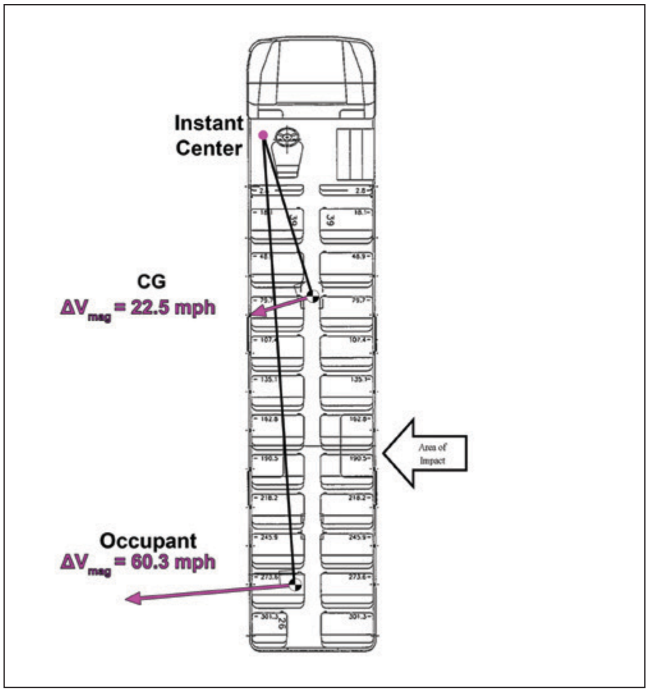

Figure 15
Diagram showing location of instant center.

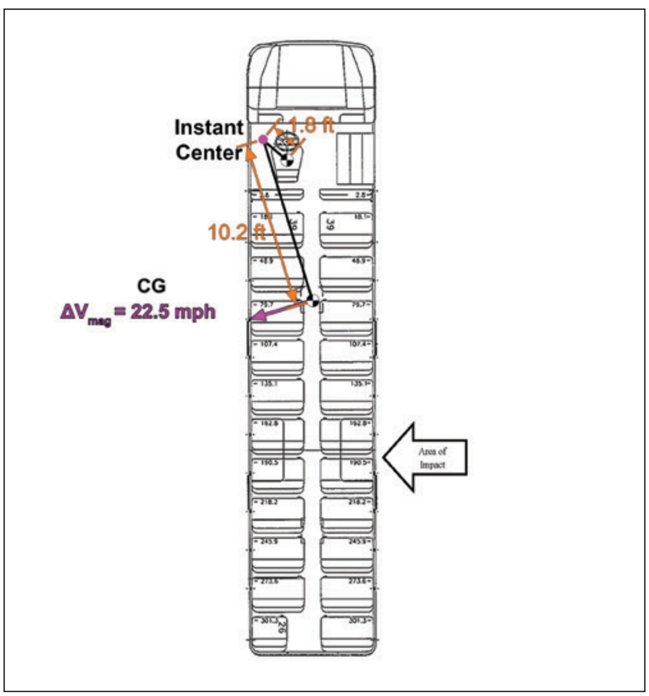

Figure 16
Diagram showing distances d_{driver} and d_{CG}.

$$\Delta V_{driver} = \frac{d_{driver}}{d_{CG}} * \Delta V_{CG} \tag{2}$$

$$\Delta V_{driver} = \frac{1.8\,ft}{10.2\,ft} * 22.5\,mph = 4.0\,mph \tag{3}$$

The direction of the delta-V vector for the bus driver's seat is perpendicular to the line drawn from the instant center to the bus driver's seat in the direction of the rotation as shown in **Figure 17**.

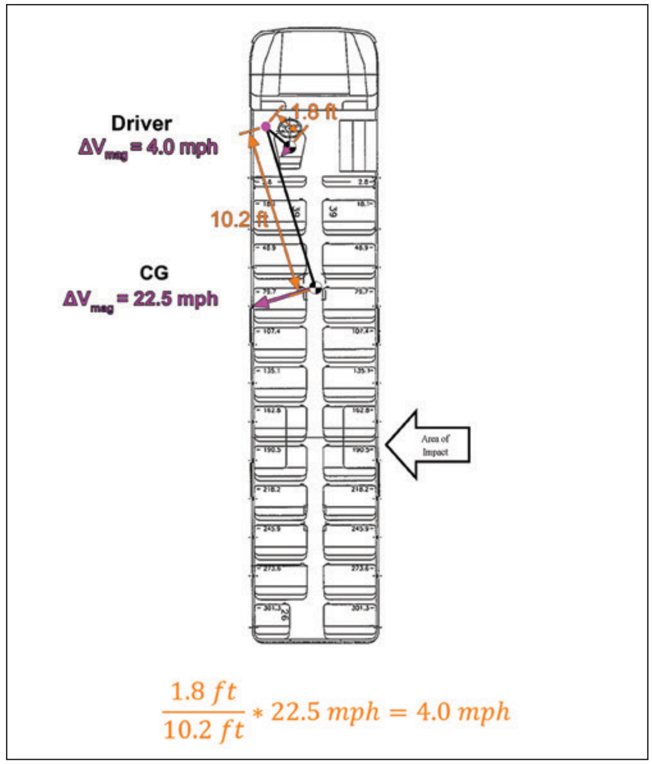

Figure 17
Direction of delta-V is perpendicular to line drawn from instant center.

Occupant Kinematics

After determining the delta-V at the seat location of the fatally injured occupant, the occupant kinematics of the fatally injured occupant were determined.

During the impact phase of the collision, the restrained portions of the occupant would have traveled in the direction of the bus seat, while the unrestrained portions of the occupant would have traveled in the opposite direction relative to the bus seat. However, during impact, the fatally injured occupant's seatbelt became unlatched, and the seat cushion became detached. Therefore, the occupant became completely unrestrained and traveled in the opposite direction relative to the bus seat (shown as dotted line in **Figure 18**).

The mean and peak accelerations sustained by the bus in the vicinity of the occupant were calculated using a Haversine model of crash pulse shown in equations (4) and (5).

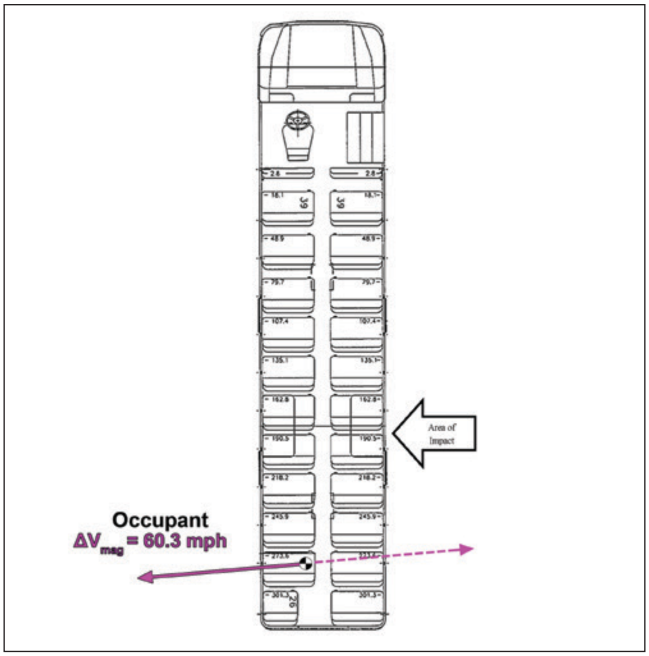

Figure 18
Direction of unrestrained occupant movement depicted by dashed line.

$$a_{occupant,mean} = \frac{\Delta V_{occupant}}{\Delta t} \tag{4}$$

$$a_{occupant,peak} = \frac{2 * \Delta V_{occupant}}{\Delta t} \tag{5}$$

The change in velocity of the occupant ($\Delta V_{occupant}$) was calculated as 60.3 mph. The impulse time (Δt) was estimated using published school bus side impact crash test data as 0.1 seconds. Through application of equations (4) and (5), the respective mean and peak accelerations of the bus in the vicinity of the occupant were calculated as approximately 27.5 g and 54.9 g.

Animation

The PC-Crash simulation data was applied to computer-generated models of the school bus and the semi within virtual space to produce traditional, linear, photo-realistic animations as well as an interactive environment of the accident.

The authors utilized a process that combines computer-generated, virtual vehicles and Google Street View Imagery (**Figure 19**) to produce linear animations of the accident that are photo-realistic in quality. The process involves matching the 3D scene's virtual camera with the background image or "backplate" (**Figure 20**) and compositing the rendered vehicles and signage over the backplate image (**Figure 21** and **Figure 22**).

Figure 19
Google Street View Imagery used as "backplate" background for animation.

Figure 20
Virtual CG Scene (blue) matched to backplate image.

Figure 21
Backplate image before compositing.

Figure 22
Still frame from composited, photo-realistic animation.

In addition to the traditional linear animations, the authors also produced an interactive virtual visualization of the accident scene. This interactive format allows the user to move around the virtual accident scene to view the accident from any vantage point in time and space. Many other parameters can also be adjusted interactively to allow the user to present a variety of views together with overlaid information, such as real-time vehicle speeds and occupant delta velocities (**Figure 23**).

Figure 23
Interactive visualization interface displaying vehicle speeds and occupant delta velocities.

Conclusion

This case study demonstrates the use of various technologies and methodologies during the reconstruction of a collision between a school bus and a semi. Such technologies and methodologies can be useful when investigating other vehicle collisions.

This paper also demonstrates the use of both analytical and graphical methods to approximate the delta-V vectors at any point on the bus. The analysis showed the delta-V near the front of the bus was only about 4 mph whereas the delta-V near the rear of the bus was approximately 70 mph. Therefore, this case study demonstrates that when investigating occupant delta-Vs in offset collisions that induce rotation in extended length passenger vehicles, such as buses or long vans, the effects of rotation cannot be neglected.

Finally, high-end rendered animations were created using data from the PC-Crash simulation. Further, an interactive animation was created, allowing the user to maneuver a virtual camera within the virtual scene. Therefore, the interactive animation allowed the user to view the accident from various vantage points around the intersection.

Bibliography

Bedford A, Fowler, W. 2008. Engineering Mechanics DYNAMICS. 5th edition. Upper Saddle River, NJ: Pearson Education, Inc. p. 476-480.

Bolte K, Jackson L, Czech B, Lack S, Barson A, Summers S. Simulations of large school bus crashes. SAE Technical Paper 2000-01-0469. Warrendale, PA: Society of Automotive Engineers; 2001.

Bolte K, Lack S, Jackson L. Large school bus side impact stiffness factors. SAE Technical Paper 2002-01-0554. Warrendale, PA: Society of Automotive Engineers; 2002.

Breen K, Anderson C. The application of photogrammetry to accident reconstruction. SAE Technical Paper 861422. Warrendale, PA: Society of Automotive Engineers; 1986.

Callahan M, LeBlanc B, Vreeland R, Bretting G. Close-range photogrammetry with laser scan point clouds. SAE Technical Paper 2012-01-0607. Warrendale, PA: Society of Automotive Engineers; 2012.

Cliff W, Montgomery D. Validation of PC-Crash – a momentum-based accident reconstruction program. SAE Technical Paper 960885. Warrendale, PA: Society of Automotive Engineers; 1996.

Cliff W, Moser A. Reconstruction of twenty staged collisions with PC-Crash's optimizer. SAE Technical Paper 2001-01-0507. Warrendale, PA: Society of Automotive Engineers; 2001.

Coleman C, Tandy D, Colborn J, Ault N. Applying camera matching methods to laser scanned three dimensional scene data with comparisons to other methods. SAE Technical Paper 2015-01-1416. Warrendale, PA: Society of Automotive Engineers; 2015.

PC-CRASH Accident-Simulation Program version 9.1. Linz, Austria; Dr. Steffan Datentechnik GmbH: 2012.

Photomodeler 2014.1.1. Vancouver, BC; Eos Systems Inc.: 2014.

Fancher P, Ervin R, Winkler C, Gillespie T. A factbook of mechanical properties of the components for single-unit and articulated heavy trucks. Report number UMTRI-86-12. Ann Arbor, MI: The University of Michigan Transportation Research Institute; 1986.

Fay R, Robinette, Deering D, Scott J. Using event data recorders in collision reconstruction. SAE Technical Paper 2002-01-0535. Warrendale, PA: Society of Automotive Engineers; 2002.

Fenton S, Kerr R. Accident scene diagramming using new photogrammetric technique. SAE Technical Paper 970944. Warrendale, PA: Society of Automotive Engineers; 1997.

Fenton S, Neale W, Rose N, Hughes W. Determining crash data using camera matching photogrammetric technique. SAE Technical Paper 2001-01-3313. Warrendale, PA: Society of Automotive Engineers; 2001.

Grimes W, Dickerson C, Smith, C. Documenting scientific visualizations and computer animations used in accident reconstruction. SAE Technical Paper 980018. Warrendale, PA: Society of Automotive Engineers; 1998.

Messerschmidt W, Muttart J. A statistical analysis of data from heavy vehicle event data recorders. SAE Technical Paper 2009-01-0880. Warrendale, PA: Society of Automotive Engineers; 2009.

Neale W, Fenton S, McFadden S, Rose N. A video tracking photogrammetry technique to survey roadways for accident reconstruction. SAE Technical Paper 2004-01-1221. Warrendale, PA: Society of Automotive Engineers; 2004.

Pepe M, Sobek J, Huett G. Three dimensional computerized photogrammetry and its application to accident reconstruction. SAE Technical Paper 890739. Warrendale, PA: Society of Automotive Engineers; 1989.

Pepe M, Sobek J, Zimmerman D. Accuracy of three-dimensional photogrammetry as established by controlled field tests. SAE Technical Paper 930662. Warrendale, PA: Society of Automotive Engineers; 1993.

Steffan H, Moser A. The Collision and trajectory models of PC-Crash. SAE Technical Paper 960886. Warrendale, PA: Society of Automotive Engineers; 1996.

Steffan H, Moser A. How to use PC-Crash to simulate rollover crashes. SAE Technical Paper 2004-01-0341. Warrendale, PA: Society of Automotive Engineers; 2004.

Switzer D, Candrlic T. Factors affecting the accuracy of non-metric analytical 3-D photogrammetry, using Photomodeler. SAE Technical Paper 1999-01-0451. Warrendale, PA: Society of Automotive Engineers; 1999.

Tandy D, Coleman C, Colborn J, Hoover T, Bae J. Benefits and methodology for dimensioning a vehicle using a 3D scanner for accident reconstruction purposes. SAE Technical Paper 2012-01-0617. Warrendale, PA: Society of Automotive Engineers; 2012.

Varat M, Husher S. Vehicle impact response analysis through the use of accelerometer data. SAE Technical Paper 2000-01-0850. Warrendale, PA: Society of Automotive Engineers; 2000.

Ziernicki R, Danaher D. Forensic engineering use of computer animations and graphics. Journal of the National Academy of Forensic Engineers. 2006;23(2):1-9.

Ziernicki R, Danaher D, Ball J. Forensic engineering evaluation of physical evidence in accident reconstruction. Journal of the National Academy of Forensic Engineers. 2007;24(2):1-10.

Ziernicki R, Pierce W, Leiloglou A. Forensic engineering usage of surveillance video in accident reconstruction. Journal of the National Academy of Forensic Engineers. 2014;31(2):9-19.

Appendix A

First equations (1) and (2) were applied to determine the semi's average velocity range over the time range of 0.263 and 0.33 seconds.

$$V_{avg,min} = \frac{d}{t_{max}} = \frac{20.8\ \text{ft}}{0.33\ s} = 63.0\ \frac{ft}{s} \tag{1}$$

$$V_{avg,max} = \frac{d}{t_{min}} = \frac{20.8\ ft}{0.263\ s} = 79.1\ \frac{ft}{s} \tag{2}$$

Next, the range of speed reduction, ΔV, due to braking was calculated using (3) and (4)

$$\Delta V_{min} = a * t_{min} = 0.319\ g * \frac{32.2\ \frac{ft}{s}}{g} * 0.26\ s = 2.7\ \frac{ft}{s} \tag{3}$$

$$\Delta V_{max} = a * t_{max} = 0.319\ g * \frac{32.2\ \frac{ft}{s}}{g} * 0.33\ s = 3.4\ \frac{ft}{s} \tag{4}$$

Finally, the impact speed range was calculated using (5) and (6)

$$V_{impact,min} = V_{avg,min} - \frac{\Delta V_{max}}{2} = 63.0\ \frac{ft}{s} - \frac{3.4\frac{ft}{s}}{2} = 61.3\frac{ft}{s} = 41.8\ mph \tag{5}$$

$$V_{impact,max} = V_{avg,max} - \frac{\Delta V_{min}}{2} = 79.1\ \frac{ft}{s} - \frac{2.7\frac{ft}{s}}{2} = 77.7\frac{ft}{s} = 53.0\ mph \tag{6}$$

Appendix B

The coordinate system used for the rigid body kinematic calculations originates at the center of gravity of the bus. The positive-x direction is oriented towards the front of the bus, the positive-y direction is oriented towards the left side of the bus, and the positive-z direction is oriented upwards.

First, the delta-V vector at the center of gravity (ΔV_{cg}) was calculated using the pre-impact velocity (V_{pre}) and post-impact velocity (V_{post}) of the school bus determined from the PC-Crash simulation data of the collision.

$$\overrightarrow{V_{pre}} = |22\ mph\ i \quad 0\ mph\ j \quad 0\ mph\ k|$$

$$\overrightarrow{V_{post}} = |15.0\ mph\ i \quad 21.7\ mph\ j \quad -0.3\ mph\ k|$$

$$\overrightarrow{\Delta V_{cg}} = \overrightarrow{V_{post}} - \overrightarrow{V_{pre}} = [-7.0\ mph\ i \quad 21.7\ mph\ j \quad -0.3\ mph\ k]$$

Next, the change in rotational velocity ($\overrightarrow{\Delta\omega}$) was determined from the PC-Crash simulation data of the collision.

$$\overrightarrow{\Delta\omega} = \left[-1.20\ \frac{rad}{s}\ i \quad -0.06\ \frac{rad}{s}\ j \quad -3.25\ \frac{rad}{s}\ k\right]$$

Next, the distance vector from the cg ($\overrightarrow{r_{A/B}}$) to the seat position of the fatally injured was determined using a scaled schematic of the school bus.

$$\overrightarrow{r_{A/B}} = |-17.4\ ft\ i \quad 1.2\ ft\ j \quad 1.45\ ft\ k|$$

Finally, the delta-V vector at the position the fatally injured occupant was sitting was determined by inputting the above quantities into the rigid body kinematics equation

$$\overrightarrow{\Delta V_{occupant}} = \overrightarrow{\Delta V_{cg}} + \overrightarrow{\Delta\omega} \times \overrightarrow{r_{A/B}}$$

Appendix B (continued)

$$\overrightarrow{\Delta\omega} \times \overrightarrow{r_{A/B}} = \begin{vmatrix} i & j & k \\ -1.2\,\frac{rad}{s} & -0.06\,\frac{rad}{s} & -3.25\,\frac{rad}{s} \\ -17.4\,ft & 1.2\,ft & 1.45\,ft \end{vmatrix}$$

$$\overrightarrow{\Delta\omega} \times \overrightarrow{r_{A/B}} = \left[3.8\,\frac{ft}{s}i \quad 58.3\,\frac{ft}{s}\,j \quad -2.5\,\frac{ft}{s}\,k\right] = [2.6\,mph\,i \quad 39.8\,mph\,j \quad -1.7\,mph\,k]$$

$$\overrightarrow{\Delta V_{occupant}} = [-7.0\,mph\,i \quad 21.7\,mph\,j \quad -0.3\,mph\,k] + [2.6\,mph\,i \quad 39.8\,mph\,j \quad -1.7\,mph\,k]$$

$$\overrightarrow{\Delta V_{occupant}} = [-4.4\,mph\,i \quad 61.5\,mph\,j \quad -2.0\,mph\,k]$$

$$\left|\Delta V_{occupant}\right| = \sqrt{(-4.4\,mph)^2 + (61.5\,mph)^2 + (-2.0\,mph)^2} = 61.7\,mph$$